GASIFICATION OF SOLID WASTE FOR SYN-GAS PRODUCTION

Synopsis of the thesis to be submitted in the partial fulfilment of the award of the degree of

Doctor of Philosophy

In

Chemical Engineering

CONTRACTOR ENDRICK DIVYAKANT
(Enrolment No: 199999911509)

Department of Chemical Engineering,
G H Patel College of Engineering & Technology
Vallabh Vidyanagar, Gujarat, India.

Under the supervision of
Dr. Alok Gautam
Professor & Dean (R & D)
Department of Chemical Engineering
Shroff S R Rotary Institute of Chemical Technology, Vataria

Gujarat Technological University
Ahmedabad-382424, Gujarat, India
JULY 2024

GASIFICATION OF SOILD WASTE FOR SYN-GAS PRODUCTION

Synopsis of the thesis to be submitted in the partial fulfilment of the award of the degree of

Doctor of philosophy

In

Chemical Engineering

CONTRACTOR ENDRICK DIVYAKANT
(Enrollment No: 199999911509)

Department of Chemical Engineering,
G H Patel College of Engineering & Technology
Vallabh Vidyanagar, Gujarat, India.

Under the supervision of
Dr. Alok Gautam
Professor & Dean (R & D)
Department of Chemical Engineering
Shroff S R Rotary Institute of Chemical Technology, Vataria

Gujarat Technological University
Ahmedabad-382424, Gujarat, India
JUNE 2024

Table of Contents

1. Abstract:

Because of the massive amounts of waste generated and the inappropriate disposal techniques, managing organic waste from industrial and agricultural sources presents serious environmental challenges. Ecological risks include soil and water contamination, air pollution, and greenhouse gas emissions result from improper treatment of these wastes. This study indicates Gasification as a feasible way to effectively address these two issues. By gasifying these organic wastes, greenhouse gas emissions are reduced and consumption on fossil fuels is lessened. Valuable syngas is produced that may be used for a variety of energy applications. By producing high-calorific syngas that is rich in CO and H_2, Gasification operations can improve combustion efficiency and provide a sustainable energy source. Gasification plants have the potential to enhance energy efficiency and yield environmental advantages in industrial environments by turning low-value feedstock into lucrative products. Further applications for the produced biochar or ash include soil amendments that increase crop yield and sequestering carbon. First, Rice Husk, pine wood, and Sugarcane Bagasse were among the agricultural wastes that were chosen for pure Gasification in the current study work. Additionally, studies have been done on the impact of the equivalence ratio on Gasification temperature, syngas composition, Lower Heating Value, Carbon Conversion Efficiency, producer gas flow rate, and other parameters. Following the tests, a variety of analytical studies, including proximate and ultimate analysis, thermogravimetric analysis, particle size analysis, Fourier transform infrared (FTIR) spectroscopy, X-ray diffraction (XRD) analysis, X-ray Fluorescence (XRF) analysis, were performed on the produced char/ash. The kinetic parametric research along with its perfect degradation model were other goals of this investigation, which used a variety of techniques including the Flynn-Wall-Ozawa (FWO), Kissinger-Akahira-Sunose (KAS), and Coats-Redfern approaches. Furthermore, industrial organic waste and agricultural waste were also co-gasified in this instance. Additionally, distinct ratios of Rice Husk and industrial organic waste have been employed for Co-Gasification. Analogously, the impact of the equivalence ratio on different parameters has been carried out and the char/ash produced has been examined using the same analytical procedures as previously indicated.

Keywords: Co-Gasification, Biomass, Syngas, Char/Ash.

2. Background and definition of the Problem:

Waste comes from a variety of places, including homes, businesses, hospitals, and agriculture. Whatever the type of garbage, there is an enormous amount of solid waste, and each type of waste poses a unique risk. For example, urban solid wastes contain decomposing materials and hazardous chemicals from hospitals, while agricultural solid wastes can contaminate groundwater and render land unusable (Zeng et al., 2021). Despite the fact that solid waste may be treated in a number of ways, the issue is getting worse every day in a nation with as many people as India. All human activities that are used and disposed of result in solid waste composition (Loan and Balanay, 2023).

Monitoring the collection, transportation, and disposal of solid waste is essential to managing such massive trash, which, if left unmanaged, poses a serious risk to the general public's health. Increased waste production is a result of a rapidly expanding population in rural and urban places alike. The employed technique might not produce the required results if there are gaps in any of the solid waste management procedures (Y. Shi et al., 2023). Moreover, it results in the disposal of wastes in open spaces, which pollutes the soil and emits an unpleasant odor, clogs drainage systems, and produces pollutants in the air when the wastes undergo combustion, which disperses a variety of diseases (Baralla et al., 2023).

The combination of material waste (wood, rose husk, as well as other agricultural waste) and their proper composition is the only focus of this proposed study because producing the best possible Syn gas is never attempted. Apparently, take the required steps to improve this strategy and attempt to reach the desired outcome. Secondly, make an effort to create a thermodynamics model for everything that would be useful for additional research.

3. Objectives and scope of work:

- Initially, design, procure and install any one type of the gasifier along with the gas clarifying system.
- Optimize the numerous parameters like amount of air requirement for the Gasification, pressure and temperature of Gasification, method involved (fluidized bed, fixed bed and other gasifier) and composition of mixed solid waste (like Biomass, agriculture waste, industrial organic waste).
- Find out the best possible characteristics of Raw material like optimum composition of mixed waste, calorific value, bulk density and other basic details which can be derived from the proximate and ultimate analysis.
- Ensure the best use of the raw material sources and Gasification technology that are available to you in order to produce the highest quality Synthesis gas (Syn Gas), which has higher concentrations of CO and H_2 in its gas composition and is meant to guide any potential reduction in emissions, including emissions of nitrogen, sulfur, and chlorine compounds.
- Detail Kinetic study of Gasification process for the given solid waste through different methodologies like model free and model fit methods.

4. Original Contribution of the research:

The primary objective of this study is to demonstrate the adaptability of the downdraft Gasification procedure by employing different biomass waste products, such as Rice Husk, Pinewood, and Sugarcane Bagasse, which are essentially organic in nature. Furthermore, following a thorough analysis of all three biomass wastes and the impact of the equivalence ratio on several Gasification parameters, Rice Husk is chosen to proceed with Co-Gasification. In the Co-Gasification process, industrial organic waste had been utilized in addition to Rice Husk, and the impact of their various amounts on the equivalence ratio was investigated. This study also focuses on the possible uses of the char/ash and syngas that are created from the Gasification process. Additionally, using a variety of analytical techniques, including elemental analysis, thermogravimetric analysis, particle size analysis, Fourier transform infrared (FTIR) spectroscopy, X-ray diffraction (XRD) analysis, and X-ray fluorescence (XRF) analysis, this study sheds light on the comparison of Rice Husk ash with co-gasified ash.

As per the authors best knowledge, a lot of research has been done on the Co-Gasification of plastic, agricultural waste, and other materials like MSW or RDF. However, since organic waste is generated by industry, there hasn't been any research done on the thermal breakdown and Co-Gasification of these residues. Its formulations may represent the first comprehensive scientific endeavours to comprehend the mixture's synergistic behaviour. Furthermore, there are several studies on the behaviour of Rice Husk and other Biomass Gasification that are available in the literature; but, to the best of the authors' knowledge, the Co-Gasification of Rice Husk and industrial organic waste, as well as the characterisation of the result, has never been reviewed before.

5. Methodology of research:

5.1 Sample Preparation:

All three biomass waste samples were collected from the local area or nearby villages in the Vallabh Vidyanagar, Gujarat region. The industrial organic waste is collected from the Nandesari Industries Association (NIA) common effluent treatment plant, Nandesari, Dist. Baroda, Gujarat, India. To obtain the same particle size, the four components were first sun dried for a week before being sieved. Rice Husk and organic waste are combined during Co-Gasification using the split and mix method to guarantee uniform distribution.

5.2 Thermogravimetric analysis (TGA):

The instruments used for TGA and DTG were 5000/2960 TA Instruments, USA. First, the apparatus was used to heat a crucible containing approximately 3 mg of sample, which heated from 30 and 700°C at a single heating rate of 10°C/min. The crucible was also fed 150 ml of nitrogen per minute (purity > 99.995).

5.3 Gasification experiments (downdraft Gasification):

In the Gasification trials, testing was conducted using a 10 kWe atmospheric pressure downdraft gasifier. The main reactor, or gasifier, is 17 inches in diameter and 14 inches tall. The Hopper is 20 inches tall overall and can hold 40 kg of weight. In order to avoid issues with feedstock channelling or bridging within the gasifier reactor, a vibration mechanism was installed on the gasifier top. The configuration of the water jet nozzle, water circulation system, and reservoir assisted in creating the necessary negative pressure to allow the producing gas to flow freely. The gas filtration system consisted of a wet scrubber, a cloth filter, and a surge tank filled with Rice Husks. A portable thermoanemometer was used to measure the gas flow rate, and temperature readings were taken utilizing corrected K (Chromel-Alumel) type thermocouples. In the current investigation, the interior temperature of the gasifier reactor was measured axially using thermocouples. The gasoline supply was located beneath the upper cover. Before the water could go through the nozzle, a water pump circulated it. By lowering pressure energy, water jet nozzles increase the kinetic energy of water. The producing gas for the nozzle section was provided by the gasifier reactor, and atmospherically compressed air was drawn in by the pressure differential. The generated gas was between 200 and 250°C (about 50°C) colder when it came out of the wet scrubber. Temperature, airflow rate, and syngas flow rate were all monitored constantly during the experiment. The gasifier configuration used in this study is shown in **Figure 1.**

5.4 Sample Analysis:

Following the successful conclusion of the trials, a sample of gas was obtained and analysed using a Sigma GC 606 gas analysis apparatus employing a packed column molecular sieve with column temperature of 80 °C, injector temperature of 200 °C, and TCD temperature of 150 °C.

Several characterisation techniques, including TGA and DTG, were employed to analyse and ascertain the char/ash features. N_2 was used as an inert gas for the procedure, which was carried out on a Mettler Toledo at a temperature of 10 °C per minute and a flow rate of 150 ml/min. Within the furnace, the sample was stored in a ceramic refractory and heated to 700 °C from room temperature. The investigation provided the authors with sufficient information to comprehend the thermal degradation of the material. For each of the three samples, TGA analysis was carried out on the char/ash and raw material.

In the 400–4000 cm^{-1} range, the functional groups found in char samples were measured with a Shimatzu (IRPrestige-21) DRS/ATR spectrometer. To identify these groups, Fourier transform–infrared (FTIR) spectra were used. Additionally, powder XRD was used to analyze the crystalline and phase variations of the char samples. A Rigaku Ultima IV Powder X-Ray Diffractometer was used to collect the data. Graphite-monochromatized Cu Kα radiation ($\lambda = 0.15406$ nm) and step scanning at $2\theta = 0.020^\circ$ per second from 5° to 80 ° were used. The elemental composition of the three materials was determined analytically using wavelength dispersive X-ray fluorescence (WD-XRF) and traditional less omnian software in the AxiosMax-Panalytical. The three char samples' particle sizes were examined using the Microtac company's Zetatrac instrument.

Primary criteria like BOD, COD, pH, acidity, alkalinity, and colour are also examined in the generated waste water.

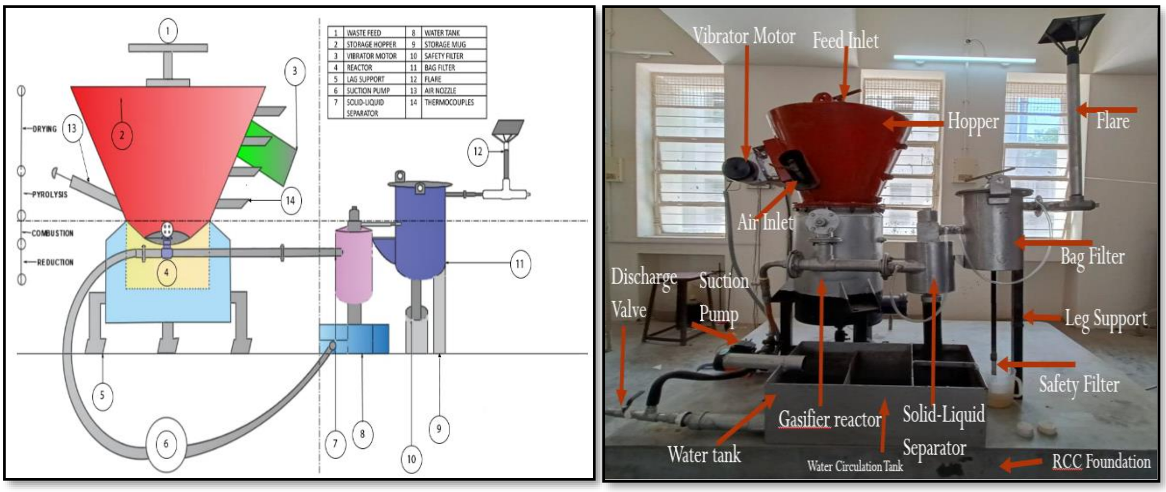

Figure 1: Lab scale equipment with layout of experimental setup.

6. Result and Discussion:

6.1 Thermogravimetric analysis (TGA/DTG)

Figure 2 shows the various proportions of the thermal degradation of Sugarcane Bagasse, Pinewood, Rice Husk, and organic waste in their raw phase. Three distinct heating rates—5, 10, and 15 °C/min—were used for the Pinewood and Sugarcane Bagasse samples, whereas 10 °C/min is maintained for the Rice Husk and organic waste samples.

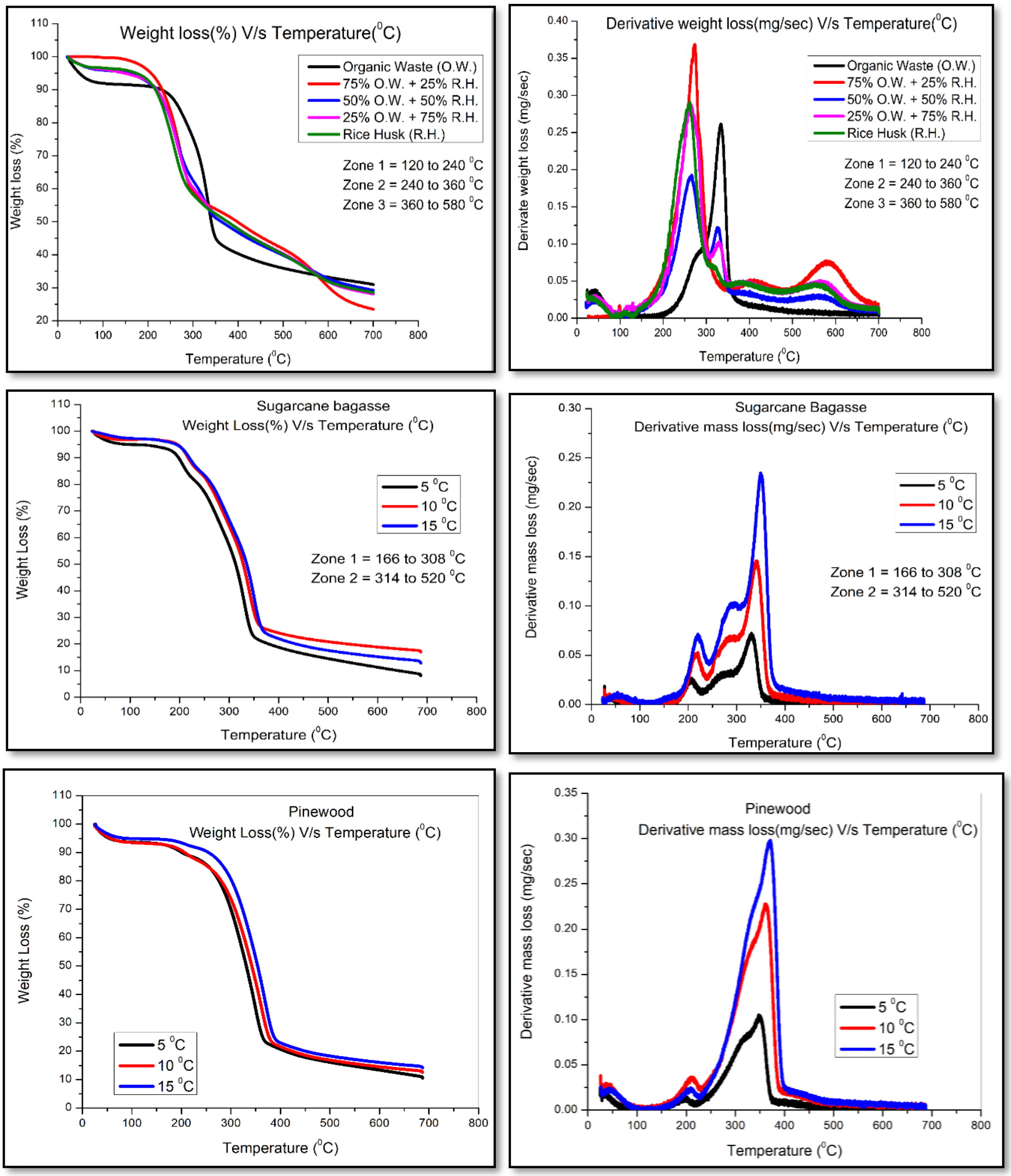

Figure 2: TGA and DTG plots as a function of temperature for the Sugarcane Bagasse, Pinewood, and ricehusk and organic waste and their different proportion.

As can be shown, the degradation patterns of Rice Husk, Sugarcane Bagasse, and Pinewood are nearly identical due to their organic content and possession of hemicellulose, lignin, and cellulose. Three zones are divided for each sample for TGA and DTG, and the range varies depending on the material. The first region is referred to as the evaporation zone or moisture removal zone, while the second zone is called hemicellulose devolatization and lignin cellulose breakdown.

Based on these figures, the temperature rise during the TG experiment, the sample's weight loss, and the total weight loss for all samples were derived and displayed in Table 2. The three distinct temperature zones are shown in Figure 2. For each of the five samples, the ranges were 120–240°C, 240–360°C, and 360–580°C, respectively. The TG-DTG curves show that each of the five samples' pyrolysis process is divided into three stages. During the drying phase, heat is absorbed by the sample material, causing the molecules to break down and this is the stage where water evaporation occurs simultaneously with the initial loss of mass occurs [Tolu Emiola-Sadiq et al. (2021)]. This phase occurred before 120°C for all five samples where the average (7-10%) mass of water vaporized. From 120°C onwards, the TG curves for all samples almost replicate the same behaviour where slow decomposing and polymerization of large molecules and their breakdown have initiated. Subsequently, during the devolatilization phase, which occurs in all five samples between 240 and 360°C, bigger molecules of Rice Husk break down into smaller ones that contain gas and condensable volatile components, while carbon and other volatile compounds are liberated. The primary phase of pyrolysis and Gasification was declared to have occurred when the percentage of weight loss in this phase was reported at 43-56%. In the last stage of the process, where char formation has been observed between 360 and 580°C for C-C and C-H bonds, an average weight loss of 37–40% has been reported.

The DTG, TG, and conversion graphs which were derived from the TGA data for the Sugarcane Bagasse from the temperature range 27-686 ^{0}C are represented in Figure 2. These graphs show the thermal analysis of Sugarcane Bagasse at different heating rates of 5,10 and 15 ^{0}C/min. It is also observed that the pattern of degradation for all three heating rates is almost similar. From these graphs, the authors decided to break the whole process into three-stage thermal decomposition and all three stages illustrate specific processes. Stage 1 is mainly the procedure of moisture removal or evaporation zone and thus this stage possessed the least interest. Here during the first stage, there was the emission of some light volatile components below 180 ^{0}C. (J. Bonilla et al. 2019) On the other hand, stage 2 is the prime decomposition process where cellulose, hemicellulose, and partially lignin decomposed. Hence, stage 2 can be called the devolatization of hemicellulose and cellulose. (Vekes Balasundram et al. 2020) Stage 3 is the step during which the decomposition of lignin occurred at the higher range of temperature > 450 ^{0}C and it is worthy to note that weight loss is not only significant but also very slow. Furthermore, it states that the residue that remains beyond 700 °C is eligible to be called a solid residual. [Moretti, M.M.de S., et al. (2016)]

Sample	Fraction Loss (%)			Overall Weight Loss (%w/w)
	Zone 1	Zone 2	Zone 3	
A	16.33	43.28	37.73	**66.35**
B	19.31	53.21	37.86	**67.03**
C	23.73	52.43	40.33	**65.98**
D	23.16	51.37	39.54	**66.55**
E	28.03	53.39	40.97	**66.68**

Table 1: Zone-wise weight loss and overall weight loss for all five samples

Sample	Heating Rate(^{0}C/min)	First Zone ^{0}C				Second Zone ^{0}C			
		T_{in}	T_{max}	T_f	Mass Loss %	T_{in}	T_{max}	T_f	Mass Loss %
Sugarcane	5	166.14	213.56	286.96	40.4011	292.38	334.32	483.68	16.0867
	10	169.18	221.52	297.24	41.4755	303.12	344.52	498.86	17.7507
	15	175.63	224.11	308.11	42.0920	314.38	352.08	520.16	21.6684

Table 2: Mass loss in % for the first and second zone of Sugarcane sample

Sample	Heating Rate (^{0}C/min)	First Zone ^{0}C				Second Zone ^{0}C			
		Tin	Tmax	Tf	Mass Loss %	Tin	Tmax	Tf	Mass Loss %
Pinewood	5	162	204.89	290.33	28.386	294.63	349.35	524.36	16.584
	10	174.97	214.39	302.25	31.234	303.12	364.32	530.47	17.381
	15	175.86	209.74	306.76	25.646	308.66	371.88	536.46	18.424

Table 3: Mass loss in % for the first and second zone of Pinewood sample

6.2 Proximate and Ultimate Analysis of the Raw samples:

Sample Details

Samples Ultimate & Proximate Analysis													
Sr. No.	**Sample ID**	**LOD (%)**	**Ash (%)**	**Volatile Matter (%)**	**Fixed Carbon (%)**	**C (%)**	**H (%)**	**N (%)**	**S (%)**	**O(%)**	**HHV (MJ/kg)**	**O/C**	**H/C**
1	**Raw Rice Husk**	4.230	18.200	61.680	15.890	38.200	5.470	1.610	0.052	54.668	14.590	1.431	0.143
2	**Raw Sugarcane Bagasse**	2.280	1.270	80.640	15.810	44.900	5.050	1.590	0.042	48.418	16.714	1.078	0.112
3	**Raw Pinewood**	3.140	0.830	80.880	15.150	48.200	5.940	1.800	0.002	44.058	16.926	0.914	0.123
4	**Organic waste**	21.750	14.320	24.120	60.190	61.900	2.220	0.100	1.080	34.700	19.523	0.561	0.036
5	**75 % R.H +25% O.W(A+)**	5.210	17.070	59.870	17.850	47.370	2.090	0.191	0.460	49.889	13.581	1.053	0.044
6	**50% R.H + 50% O.W(B+)**	6.930	16.320	47.810	28.940	54.520	1.980	0.258	0.643	42.599	16.083	0.781	0.036
7	**25% R.H + 75% O.W(C+)**	8.130	18.970	38.310	34.590	61.790	2.730	0.269	0.912	34.299	19.230	0.555	0.044
8	**60% R.H + 40% O.W(D+)**	6.430	16.940	51.190	25.440	50.160	2.550	0.170	0.533	46.587	20.313	0.929	0.051

Table 4: General characterisation and elemental analysis of raw feedstock.

Table 4 displays elemental analysis and general characteristics for several feedstocks. It has been observed that apart from organic waste all other raw samples have <10% moisture content which shows the best suitability for the Gasification process. Moreover, there is less ash and a higher volatile content in the biomass waste samples. More fuel ignition is shown by reduced ash, which means biomass is more volatile. Increased ash content leads to reduced energy conversion, costly processing expenses, ineffective combustion, and disposal problems. [Pankaj Parmar, et al. 2023] Additionally, it is noted that for samples A+ through D+, the concentration of organic waste rises from 25% to 75%, resulting in an increase in fixed carbon, LOD, and carbon. This is because organic waste has the highest fixed carbon and carbon content of any waste. Furthermore, it has been observed that the value of the ash content decreases as it approaches 75% of the concentration of organic waste, having previously been raised to 60%.
Using Dulong's formula, the higher heating value (gross calorific value) of each char sample was computed as follows:

$$HHV\left(\frac{MJ}{kg}\right) = \left[338.2 * C\% + 1442.8 * \left(H\% - \frac{O\%}{8}\right)\right] * 0.001$$

6.3 Kinetic Analysis

6.3.1 Determination of apparent activation energy

Examining the behavior of each sample utilized in the Gasification experiments' thermal degradation is the main goal of this investigation. Because of this, the Rice Husk and organic waste, in varying proportions, were first chosen for TGA analysis at a constant heating rate of 10 °C/min. To determine the various kinetic parameters, such as apparent activation energy, R2, and order of reaction, both the direct Arrhenius technique and the coats redfern method were used. The table showed all of the calculated values for every parameter. Next, three distinct heating rates—5, 10, and 15 °C/min—were selected to simulate Sugarcane Bagasse and Pinewood, and corresponding kinetic parametric studies were carried out for both materials. The Flynn-Wall-Ozawa (FWO) method is utilized for the sugarcane sample, while the Kissinger-Akahira-Sunose (KAS) method is utilized for the Pinewood sample. Tables have been created using the computed findings from both approaches for both samples.
The equation which were used in this study are as following:

$\frac{d\alpha}{dt} = -Ae^{-\left(\frac{E_a}{RT}\right)} f(\alpha)$……(Direct Arrhenius equation)…………………………………...(1)

$ln\left\{\frac{1-(1-a)^{1-n}}{T^2(1-n)}\right\} = \ln\left\{\frac{AR}{\beta E_a}\right\} - \frac{E_a}{RT}$ (For n ≠ 1) &

$\ln\left\{\frac{-ln(1-a)}{T^2}\right\} = \ln\left\{\frac{AR}{\beta E_a}\right\} - \frac{E_a}{RT}$ (For n = 1)… (Coats Redfern Equation)……………..… (2)

$\ln\beta = \frac{AE_\alpha}{g(\alpha)R} - 5.330 - 1.052\frac{E_\alpha}{RT}$………(FWO Equation)…………………..………..…(3)

$ln\left(\frac{\beta_i}{T_{\alpha i}^2}\right) = ln\left(\frac{A_\alpha R}{E_\alpha g_\alpha}\right) - \frac{E_\alpha}{RT_{\alpha i}}$……(KAS Equation)…………………………..…………(4)

FWO method						
α	**First Zone**			**Second Zone**		
	E(KJ/mol)	**R^2**	**ln A**	**E(KJ/mol)**	**R^2**	**ln A**
0.1	86.26	0.9918	24.3754	87.49	0.9973	23.1532
0.2	94.72	0.99	27.7425	99.88	0.9989	27.1513
0.3	82.28	0.9964	23.4076	107.96	0.9951	29.6923
0.4	80.51	0.9968	22.3097	108.61	0.9996	30.3104
0.5	78.48	0.9997	21.3893	109.52	0.9913	30.4529
0.6	99.96	0.9953	28.1043	104.01	0.996	29.0839
0.7	87.63	0.9932	23.9662	115.36	0.9972	32.4036
0.8	94.74	0.992	25.9958	110.76	0.9937	31.3153
0.9	91.99	0.9879	24.9625	76.33	0.7899	21.4031
avg	88.5123	0.9936	24.6948	102.32	0.9732	28.3296

Table 5: Activation energy, R^2 and ln A obtained by FWO model-free method for Sugarcane Bagasse

KAS method						
α	**First Zone**			**Second Zone**		
	E(KJ/mol)	**R^2**	**lnA**	**E(KJ/mol)**	**R^2**	**lnA**
0.1	111.44	0.9992	20.75482	223.29	0.9986	43.25407
0.2	70.42	0.9029	10.32681	214.60	0.9993	41.33934
0.3	94.28	0.8785	16.15202	213.69	0.9993	40.96078
0.4	123.77	0.9225	22.96192	208.32	0.9987	39.63017
0.5	135.16	0.9778	25.42902	201.43	0.9999	38.04108
0.6	147.79	0.9906	28.13733	196.60	0.9987	36.94144
0.7	153.93	0.9966	29.35032	188.78	0.9994	35.23478
0.8	160.30	0.9984	30.67782	181.31	0.9992	33.65597
0.9	157.72	0.9931	29.96926	513.58	0.9924	93.03633
avg	128.3131	0.962178	23.75104	237.9559	0.998389	44.67711

Table 6: Activation energy, R^2 and ln A obtained by KAS model-free method for Pinewood

Finally, pertinent decomposition processes were found using a Criado differential-integral master plot.

6.3.2 Determination of the most probable reaction model

The "master plots," or reference theoretical curves, are employed in a variety of studies that analyze experimental data [J.M. Criado 1977]. Criado et al. 1977 published a technique for determining the reaction mechanism of the samples at a constant heating rate. It makes use of the reduced time plot concept for α against t/tα, which was put forth by Ozawa [27], where tα is the time it takes to reach a given value of α, which is typically 0.5 to 0.9. Here, a heating rate of 5,10 and 15 °C per minute was chosen at random.

Theoretical curve: $$\frac{Z(\alpha)}{Z(0.5)} = \frac{f(\alpha)g(\alpha)}{f(0.5)g(0.5)} \quad \text{.............................. (5)}$$

Experimental curve (Master curve): $$\frac{Z(\alpha)}{Z(0.5)} = \left(\frac{T_\alpha}{T_{0.5}}\right)^2 \frac{(d\alpha|dt)_\alpha}{(d\alpha|dt)_{0.5}} \quad \text{........................ (6)}$$

Plotting the $\frac{Z(\alpha)}{Z(0.5)}$ vs. α graph for various mechanisms allowed for the creation of theoretical curves. The experiment's $\frac{Z(\alpha)}{Z(0.5)}$value was obtained using known activation energies, and it was overlapped to ensure that the reaction mechanism best fit the data. Figure shows both zone plots for the Sugarcane Bagasse and Pinewood samples.

The obtained Sugarcane Bagasse experimental curve for zone one corresponds to the m3 reaction mechanism, whereas zone two follows the m11 reaction mechanism. In contrast, the experimental curve for the Pinewood sample follows the m3 reaction mechanism in zone one and the m11 reaction mechanism in zone two.

No.	**Function name**	**Mechanisms**	**f(α)**	**g(α)**
m1	Jander equation	Diffusion, 3D (spherical symmetry)	$3/2(1-\alpha)^{2/3}[1-(1-\alpha)^{1/3}]^{-1}$	$[1-(1-\alpha)^{1/3}]^{1/2}$
m2	G–B equation	Diffusion, 3D (column symmetry)	$3/2[(1-\alpha)^{-1/3}-1]^{-1}$	$1-2\alpha/3-(1-\alpha)^{2/3}$
m3	Anti–Jander equation	Diffusion, 3D	$3/2(1+\alpha)^{2/3}[(1+\alpha)^{1/3}-1]^{-1}$	$[(1+\alpha)^{1/3}-1]^2$
m4	Z–L–T equation	Diffusion, 3D	$3/2(1-\alpha)^{4/3}[(1-\alpha)^{-1/3}-1]^{-1}$	$[(1-\alpha)^{-1/3}-1]^2$
m5	Avrami–Erofeev Equation	Random nucleation and nuclei growth, n=3	$3(1-\alpha)[-\ln(1-\alpha)]^{2/3}$	$[-\ln(1-\alpha)]^{1/3}$
m6	Avrami–Erofeev Equation	Random nucleation and nuclei growth, n=2	$2(1-\alpha)[-\ln(1-\alpha)]^{1/2}$	$[-\ln(1-\alpha)]^{1/2}$
m7	Avrami–Erofeev Equation	Random nucleation and nuclei growth, n=3/2	$3/2(1-\alpha)[-\ln(1-\alpha)]^{1/3}$	$[-\ln(1-\alpha)]^{2/3}$
m8	Avrami–Erofeev Equation	Random nucleation and nuclei growth, n=4/3	$4/3(1-\alpha)[-\ln(1-\alpha)]^{1/4}$	$[-\ln(1-\alpha)]^{3/4}$
m9	Geometrical contraction	Shrinkage geometric shape ((column symmetry)	$3(1-\alpha)^{2/3}$	$1-(1-\alpha)^{1/3}$
m10	Geometrical contraction	Shrinkage geometric shape, (spherical symmetry)	$2(1-\alpha)^{1/2}$	$1-(1-\alpha)^{1/2}$
m11	Reaction order n=2	Chemical reaction	$(1-\alpha)^2$	$(1-\alpha)^{-1}-1$
m12	Reaction order n=1	Chemical reaction	$(1-\alpha)$	$-\mathrm{Ln}(1-\alpha)$
m13	Reaction order n=3	Chemical reaction	$(1-\alpha)^3$	$((1-\alpha)^{-2}-1)/2$

Table 9: Different degradation mechanisms with f(α) and g(α).

Temp.	120 to 240 ^{O}C			240 to 360 ^{O}C			360 to 700 ^{O}C		
Sample A									
Zone	**1**			**2**			**3**		
Method	**DA**			**DA**			**DA**		
n	1.9	2	2.1	0.6	0.7	0.8	2.8	2.9	3
R^2	0.62	0.6201	0.6199	0.9585	0.9519	0.9394	0.648	0.6515	0.6548
Ea/R	9033.9	9278.3	9522.8	9234.4	10185	11136	14759	15382	16004
Ea	75.1078446	77.139786	79.1725592	76.7748016	84.6781	92.5847	122.706326	127.8859	133.05726
Intercept	17.594	18.32	19.046	12.487	14.243	15.999	17.279	18.203	19.128
A	218749525	452110833	934421250.7	1324357.392	7667015	44386144	159640970	402191102	1014272975
Sample B									
Zone	**1**			**2**			**3**		
Method	**DA**			**DA**			**DA**		
n	0.2	0.3	0.4	2.8	2.9	3	2.8	2.9	3
R^2	0.9192	0.9195	0.9177	0.9132	0.9151	0.9168	0.648	0.6515	0.6548
Ea/R	6733.4	6983.1	7232.8	26736	27957	29179	14759	15382	16004
Ea	55.9814876	58.057493	60.1334992	222.283104	232.434	242.594	122.706326	127.8859	133.05726
Intercept	10.446	11.043	11.639	47.429	49.745	52.062	17.279	18.203	19.128
A	172032.366	312524.43	567183.3576	1.98E+21	2.01E+22	2.04E+23	159640970	402191102	1014272975
Sample C									

Zone	1			2			3		
Method	**DA**			**DA**			**DA**		
n	0.1	0.2	0.3	2.8	2.9	3	2.3	2.4	2.5
R^2	0.977	0.9676	0.9568	0.7542	0.755	0.7558	0.7229	0.7237	0.7244
Ea/R	5643.1	5916.5	6189.9	27466	28586	29705	14047	14746	15444
Ea	46.9167334	49.189781	51.4628286	228.352324	237.664	246.967	116.786758	122.5982	128.40142
Intercept	7.7961	8.4789	9.1616	47.898	49.999	52.1	15.644	16.66	17.677
A	12155.5108	24060.768	47621.41873	3.17E+21	2.59E+22	2.12E+23	31122385.6	85963893	237680505
Sample D									
Zone	**1**			**2**			**3**		
Method	**DA**			**DA**			**DA**		
n	0.1	0.2	0.3	2.8	2.9	3	2.3	2.4	2.5
R^2	0.8708	0.8585	0.8455	0.7894	0.7915	0.7934	0.7469	0.7468	0.7466
Ea/R	4787.2	5051	5314.9	26467	27598	28730	14802	15531	16259
Ea	39.8007808	41.994014	44.18808	220.046638	229.4498	238.8612	123.06383	129.12473	135.177326
Intercept	5.9267	6.588	7.2494	46.475	48.612	50.748	16.627	17.684	18.74
A	1874.576249	3631.63381	7036.3012	7.63E+20	6.47E+21	5.48E+22	83173380.8	239350105	688095306
Sample E									
Zone	**1**			**2**			**3**		
Method	**DA**			**DA**			**DA**		
n	**0.9**	**1**	**1.1**	**0.1**	**0.2**	**0.3**	**2.7**	**2.8**	**2.9**
R^2	0.9177	0.9093	0.9008	0.8832	0.7706	0.5589	0.7413	0.7416	0.7417

Ea/R	9768.7	10024	10280	5128.6	4007.3	2886.1	17663	18400	19137
Ea	81.2169718	83.339536	85.46792	42.6391804	33.31669	23.99504	146.85018	152.9776	159.105018
Intercept	17.225	17.851	18.477	13.086	10.956	8.8256	20.882	21.953	23.025
A	151248980.2	282853008	528967691	2410724.572	286484	34031.37	5860131687	1.71E+10	49957471600

Table 7: Direct Arrhenius method for Rice Husk, organic waste and their different proportion.

Temp.	**120 to 240 ^{O}C**			**240 to 360 ^{O}C**			**360 to 700 ^{O}C**		
Sample A									
Zone	**1**			**2**			**3**		
Method	**CR**			**CR**			**CR**		
n	0	0.1	0.2	1.2	1.3	1.4	1.5	1.6	1.7
R^2	0.9382	0.8953	0.8243	0.9481	0.9469	0.9441	0.8764	0.8749	0.8715
Ea/R	555.49	509.6	458.16	15617	16166	16742	6442.8	6847.7	7266.8
Ea	4.6183	4.2368	3.8091	129.84	134.4	139.19	53.565	56.932	60.416
Intercept	13.656	13.489	13.308	13.588	14.601	15.662	4.9137	4.3194	3.705
A	2.40E+09	1.80E+09	1.40E+09	6.20E+10	1.80E+11	5.30E+11	236.62	455.641	893.824
Sample B									
Zone	**1**			**2**			**3**		
Method	**CR**			**CR**			**CR**		
n	0	0.1	0.2	2.5	2.6	2.7	1.5	1.6	1.7
R^2	0.9994	0.9992	0.9986	0.955	0.955	0.9546	0.8758	0.8757	0.8738
Ea/R	5509.8	5610.5	5714.7	23545	24614	25695	6852.4	6450.7	7268.1
Ea	45.808	46.646	47.512	195.75	204.64	213.63	56.971	53.631	60.427
Intercept	1.8005	1.5586	1.3086	30.354	32.363	34.396	4.3174	4.9073	3.7075
A	166745	133310	105750	1.80E+18	1.40E+19	1.10E+20	2569424	4363050	1480941
Sample C									

Zone	1			2			3		
Method	**CR**			**CR**			**CR**		
n	0	0.1	0.2	2	2.1	2.2	1.4	1.5	1.6
R^2	0.7993	0.7935	0.787	0.9075	0.903	0.8982	0.9172	0.9174	0.9154
Ea/R	1164.2	1252.4	1344.9	17336	18196	19074	7635.4	8074.1	8530
Ea	9.6792	10.412	11.181	144.13	151.28	158.58	63.481	67.128	70.918
Intercept	10.479	10.253	10.016	18.288	19.892	21.529	3.6836	3.05	2.3922
A	2.10E+08	1.80E+08	1.50E+08	7.60E+12	4.00E+13	2.10E+14	1519039	852437	466486
Sample D									
Zone	**1**			**2**			**3**		
Method	**CR**			**CR**			**CR**		
n	0	0.1	0.2	2	2.1	2.2	1.3	1.4	1.5
R^2	0.7682	0.7623	0.7555	0.9204	0.9196	0.9181	0.9229	0.9253	0.9252
Ea/R	1042.7	1126.7	1214.9	17072	17944	18835	7594	8034	8493
Ea	8.669	9.3674	10.101	141.94	149.19	156.59	63.137	66.795	70.611
Intercept	10.739	10.521	10.294	18.056	19.692	21.361	3.8387	3.2044	2.5428
A	2.40E+08	2.10E+08	1.80E+08	5.90E+12	3.20E+13	1.80E+14	1764277	989817	539952
Sample E									
Zone	**1**			**2**			**3**		
Method	**CR**			**CR**			**CR**		
n	0	0.1	0.2	2	2.1	2.2	1.5	1.6	1.7
R^2	0.7749	0.7694	0.7633	0.8995	0.8989	0.8977	0.9248	0.9226	0.9187
Ea/R	1720.1	1805.5	1894.6	16019	16892	17783	8430.3	8915.2	9417.5
Ea	14.301	15.011	15.752	133.18	140.44	147.85	70.09	74.121	78.297
Intercept	9.5175	9.3038	9.0816	16.43	18.074	19.751	2.5677	1.8691	1.1462
A	1.20E+08	9.90E+07	8.30E+07	1.10E+12	6.00E+12	3.40E+13	549479	288962	148147

Table 8: Coats – Redfern method for Rice Husk, organic waste and their different proportion.

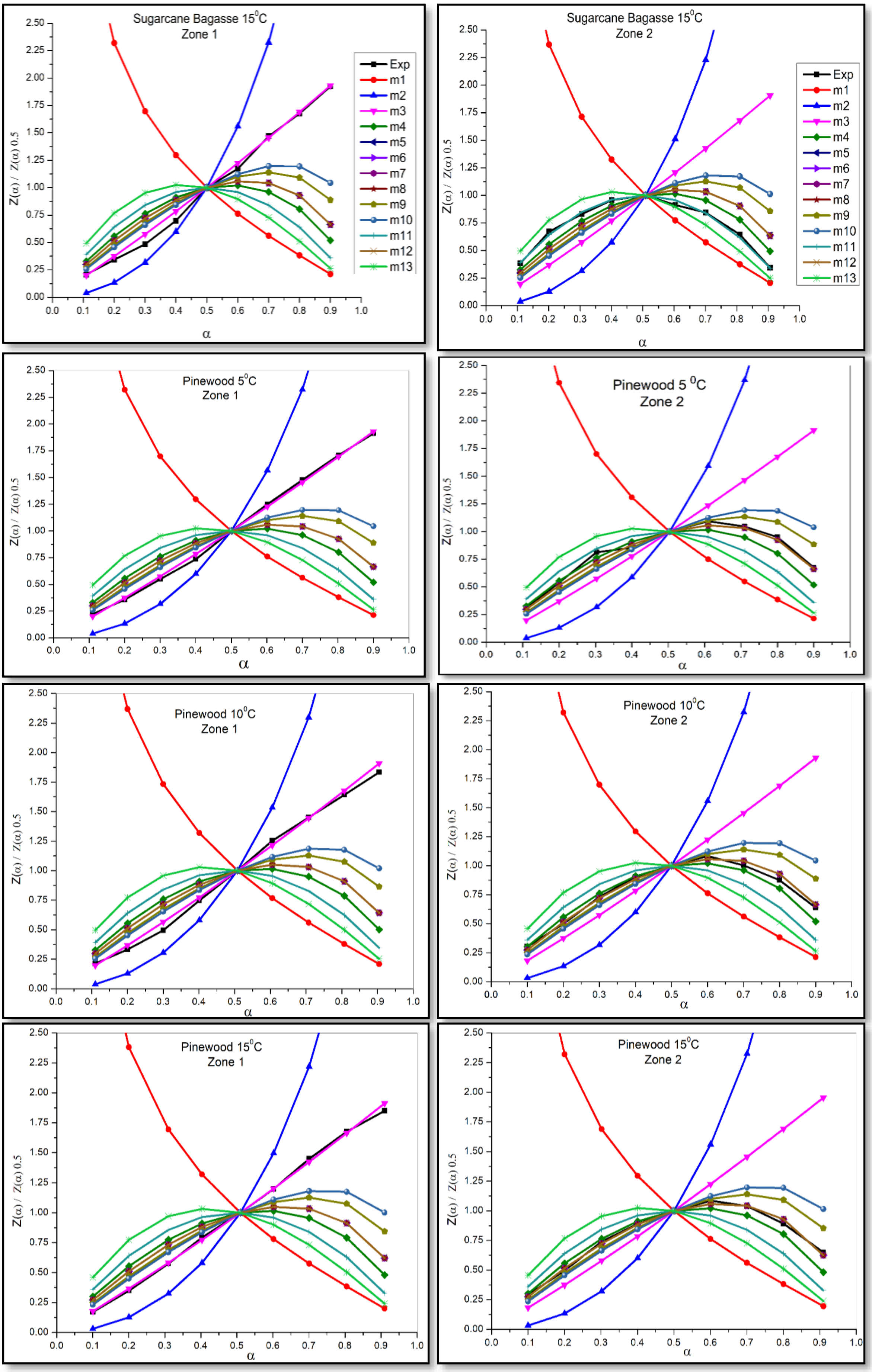

Figure 3: Sugarcane Bagasse and Pinewood criado plots for both zones for 5, 10 and 15 ^{0}C/min.

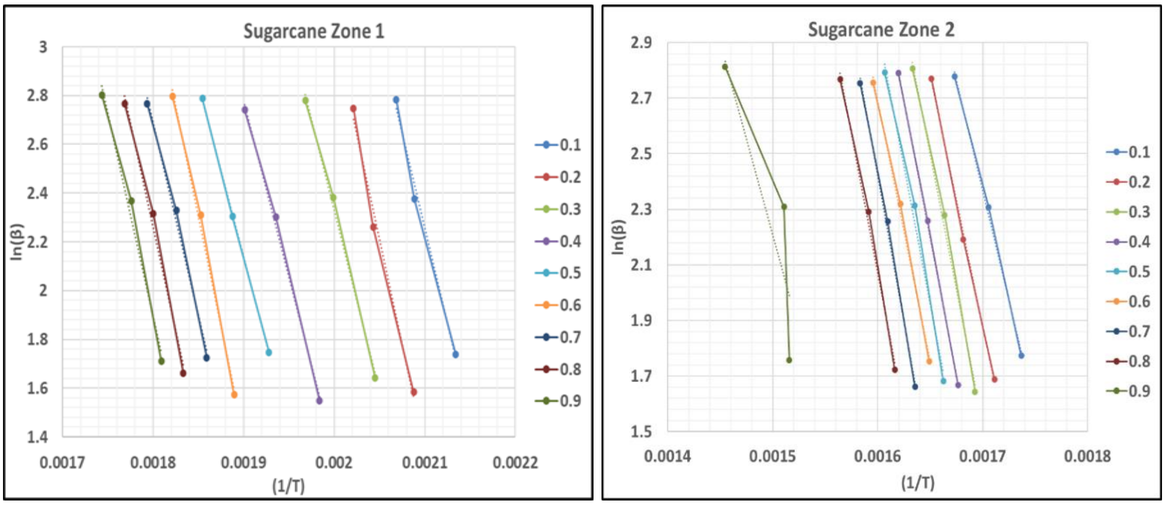

Figure 4: FWO method graphs for the Sugarcane Bagasse sample

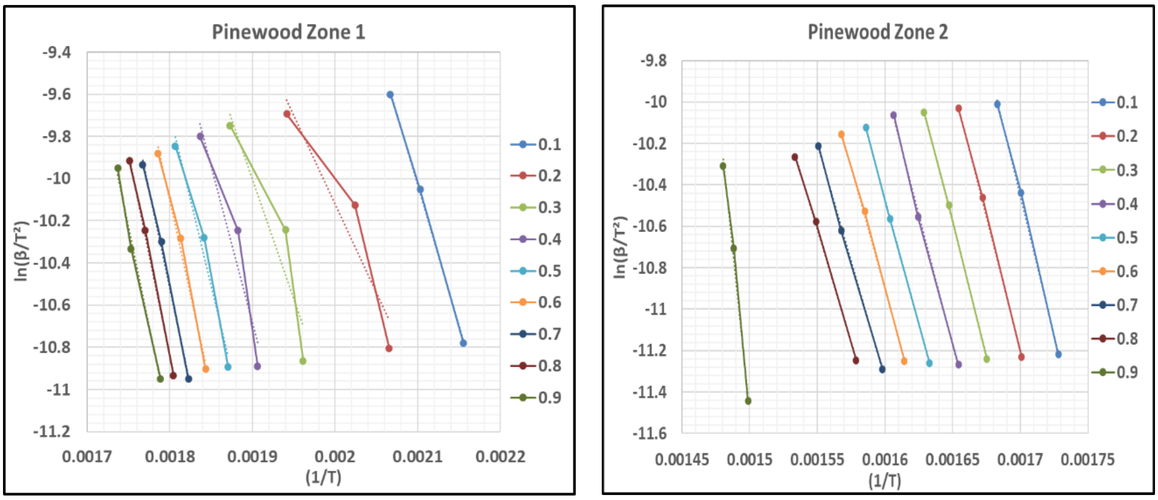

Figure 5: KAS method graphs for the Pinewood sample.

6.4 Gasification experiments:

Research has shown that the region where Gasification works best is between 0.2 and 0.4 for the Equivalence Ratio (ER) [A. A. P. Susastriawan, Harwin Saptoadi & Purnomo 2019]. The pyrolysis reaction takes primacy when the ER is less than 0.2, whereas the combustion process usually takes precedence when the ER is more than 0.4. Below is a list of a number of operational and functional parameters, including the rates of air and fuel consumption, the temperature at which Gasification takes place, the types of producer gases, the heating value, the gas output, and the cold gas efficiency.

6.4.1 The impact of E.R. on the temperature during Gasification, fuel consumption rate, and input air flow rate and gas composition.

First, a pure Rice Husk sample was obtained, and several parameters were checked against different equivalence ratio values. Four distinct equivalence ratios—0.18, 0.2, 0.25, and 0.29 — were chosen in this instance. The temperature of Gasification, air pressure, and fuel consumption rate are shown in the figure. The E.R. values for Pinewood are 0.25, 0.29, 0.35, and 0.37, and for Sugarcane Bagasse, they are 0.15, 0.18, 0.22, and 0.27.

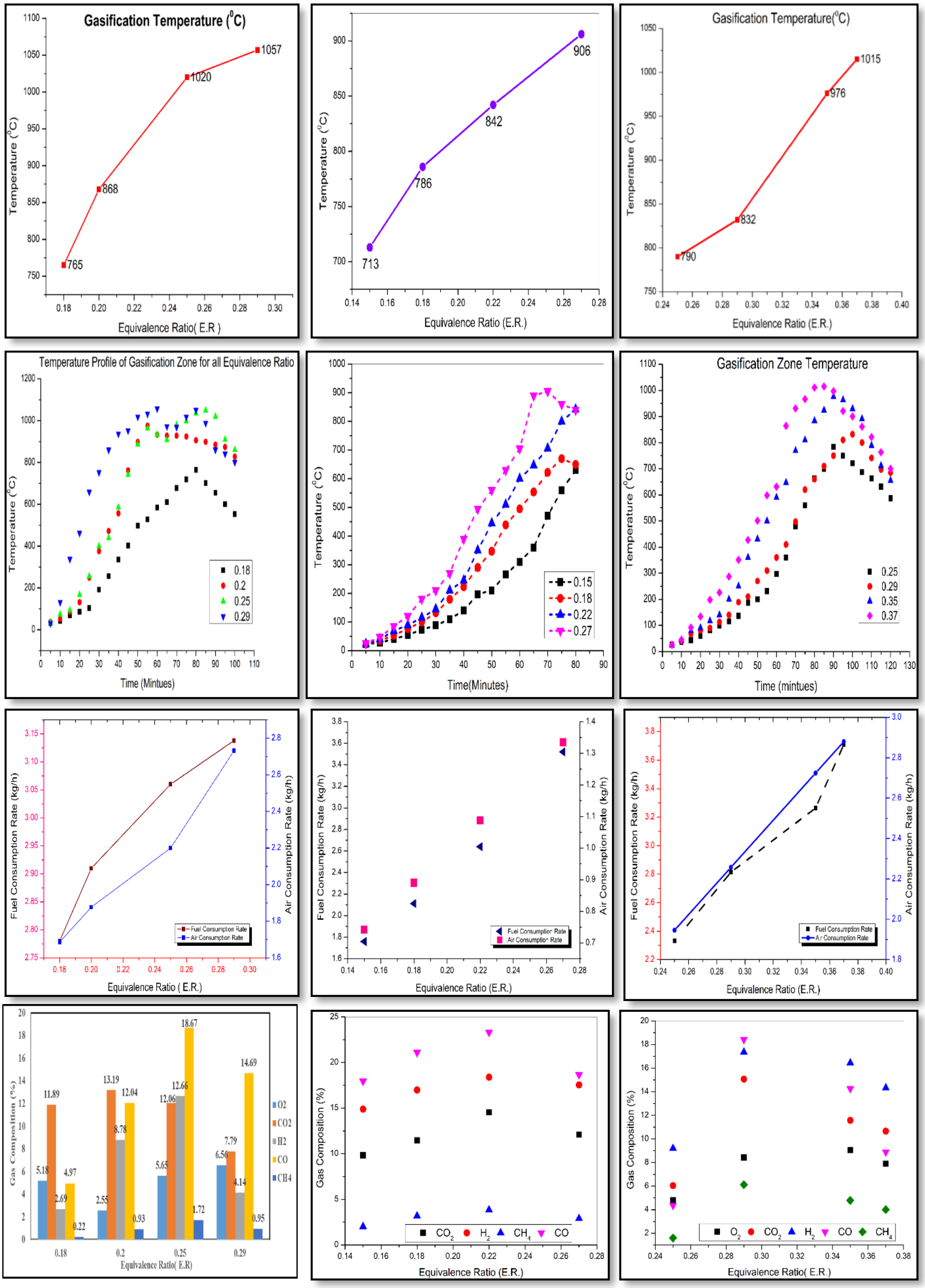

Figure 6: Gasification temperature, Gasification zone temperature, air and fuel consumption and gas compositions for Rice Husk, Sugarcane Bagasse and Pinewood samples.

Furthermore, the temperature at which Gasification occurs is demonstrated to increase as E.R. increases. Gasification gave way to combustion as a result of more oxygen being available for fuel ignition at higher E.R. 765 °C was the lowest temperature recorded at E.R 0.18, while 1057 °C was the highest temperature recorded at E.R 0.29. The reduced temperature prevented ER 0.18 from producing the Gasification zone as intended. Since lignin, a refractory component of biomass, does not gasify effectively at lower temperatures, a minimum Gasification temperature within the range of 800–900 °C is preferred for the thermal Gasification of biomass made from lignocellulosic materials. [Jahromi R, (2020) & Motta, I. L. (2019)] It has been identified that the Gasification temperature of Pinewood increases simultaneously with the equivalence ratio. It reflects that when there is more fuel compared to the stoichiometric ratio a higher Gasification temperature is required for the complete combustion. The result shows that the equivalent ratio lies between 0.25 when the Gasification temperature is 790℃. The ER becomes 0.29 at a Gasification temperature of 832℃ for Pinewood. Furthermore, the values of ER recorded 0.35 and 0.37 respectively for the corresponding Gasification temperature of 976 and 1015℃. It reflects that the ER value for Pinewood combustion increases when the Gasification temperature goes high. The temperature at which Gasification occurs is an important process choice. In the thermal Gasification of biomass derived from lignocellulosic materials, a minimal Gasification temperature in a range of 800–900 °C is preferred because lignin, a refractory ingredient in biomass, does not gasify well at lower temperatures. [Kawale, H. D., & Kishore, N. 2020] Higher ER has an impact on higher oxygen availability for syngas compositions. The primary reason for this happens is which higher temperatures favors the endothermic reaction, which converts CO_2 into CO. However, after ER reached 0.29, the percentage of CO reached 14.69%, which is because more CO_2 was converted by the excess air. As ER increased from 0.18 to 0.25, the amount of CO increased from 4.97% to 18.67%. The rate of generated gas in air Gasification is increased by raising the equivalence ratio. [Havilah, P.R.; 2022] The concentrations of carbon monoxide (CO) and hydrogen (H_2) surged from 17.95 to 23.31% and 14.89 to 18.39%, respectively, as the ER climbed from 0.15 to 0.22, according to the data. Findings also showed that a higher ER causes a higher amount of oxygen to be available for biomass oxidation, which raises the temperature of the reactor. High reactor temperatures favor CO and H_2 increment trends, which are ascribed to the impact of endothermic reactions (methane and water-gas reforming). [Awais, M.,2020] Then after concentration of both the gases decreased. CO content steadily declined from 23.31 to 18.66, and H_2 slightly decreased from 18.39 to 17.54 as ER climbed gradually from 0.22 to 0.27. It is apparent that as the E.R. value rises from 0.25 to 0.29, the levels of H_2 and CH_4 decrease as the E.R. value falls from 0.29 to 0.37. A comparable pattern was also observed for CO and CO2. The CO_2 and CO values for the 0.25 E.R. are 6.04 and 4.37, respectively. These values rise to 15.07 and 18.42% at the 0.29 E.R., then they further decrease as the E.R. value increases, reaching their lowest values at 10.66% and 8.89%, respectively. The oxidation reaction (the formation of CO_2) was aided by the maximum airflow, which naturally raised the ER and increased the CO_2 content while lowering the amounts of CO, CH_4, and H_2. The reduction in H_2 and CO can be attributed to the oxidation processes of H_2 and CO, which lead to more oxidation to H_2O and CO_2. When the E.R. value grows, the values of CH_4 decrease. (Svishchev, D. 2022) The smallest concentration of CH4 was recorded at 0.25 E.R., and it was just 1.6. Its highest level was attained at E.R. 0.29, or 6.12%. These discrepancies could result from tars thermally breaking as ER increases. Tar broke down into CO and other energy components as ER increased, strengthening the tar-cracking processes. As was shown, the process moved closer to the combustion zone as ER grew, which resulted in a drop in the quality of the syngas that was produced. (Yan cao, et.al 2021)

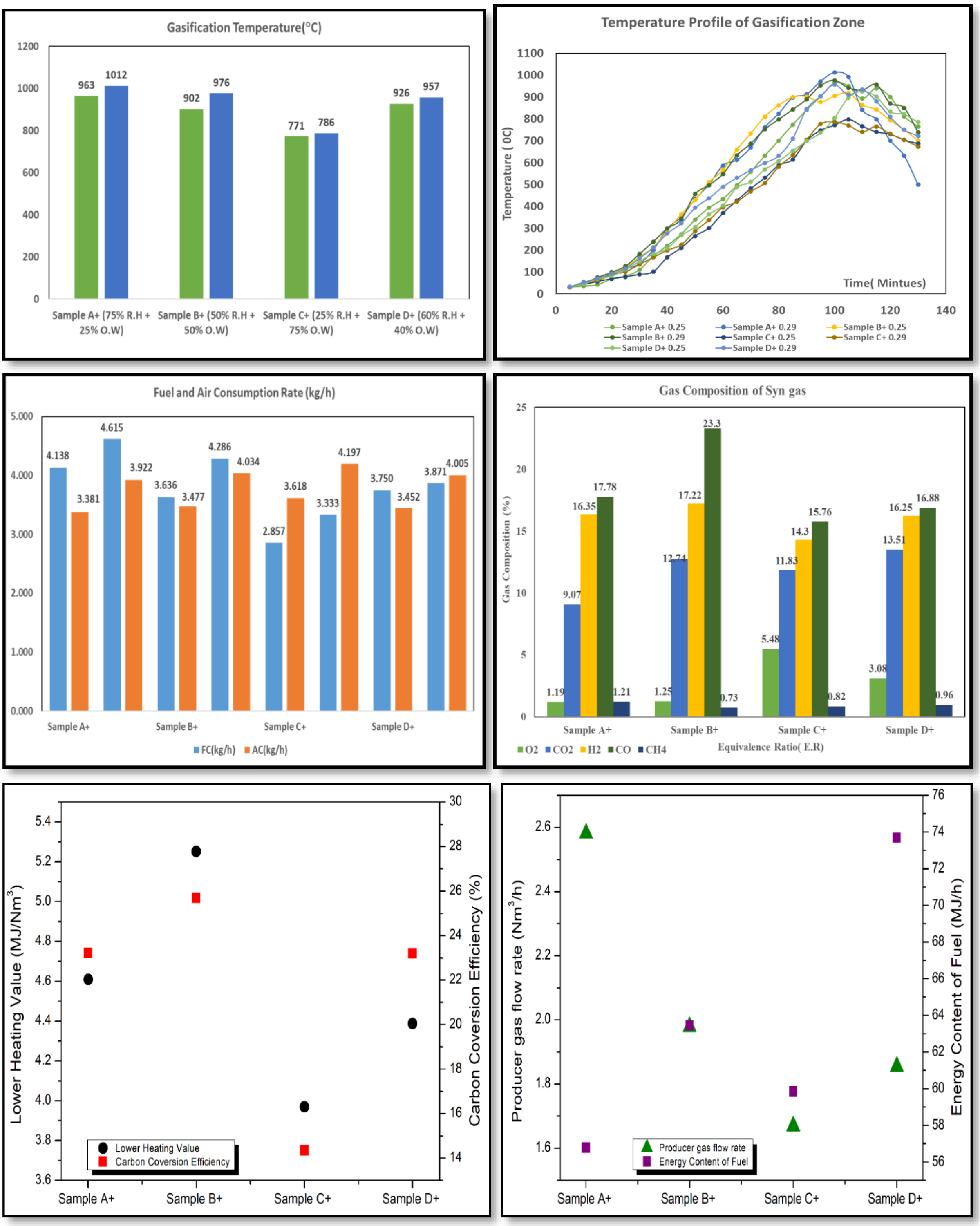

Figure 7: Gasification temperature, Gasification zone temperature, air and fuel consumption and gas compositions for Rice Husk and organic waste different proportion samples.

6.4.2 Effect of Equivalence Ratio on Lower Heating Value, Carbon Conversion Efficiency, Energy content of Fuel, Flow rate of producer gas:

Figure 8 illustrates the relationship among lower heating value and carbon conversion efficiency to equivalence ratio. Figure 8 demonstrates how the lower heating value and the carbon conversion efficiency rose as the value of ER climbed from 0.18 to 0.25. The characteristics LHV and CCG have peak values of 4.50181 MJ/Nm^3 and 34.27%, respectively, at ER 0.25. At the ER 0.29, both values decline by 24.88% and 2.740 MJ/Nm^3 his is due to the fact that at ER 0.29, concentrations of flammable gases, such as H_2, dropped while those of non-combustible gases, such as N_2 and CO_2, increased. These findings are consistent with the studies carried out by [Zhao, S.2019] The performance efficiency of biomass energy depends on the lower heating value and carbon conversion efficiency. A perfect balance between heating value and emission should be maintained to identify the most effective ER value and Gasification temperature. The lower heating value of Pinewood Gasification reached a peak of 6.5 MJ/Nm^3 at 832℃ (ER value 0.29). However, the carbon conversion efficiency also was at their peak of 33% compared to other ER values. The lower heating value became 4.21 MJ/Nm^3 and carbon conversion efficiency was 20% at 1015℃ (ER: 0.37) which was more balanced. There is a documented decline in both heating value and carbon conversion efficiency at the 0.29 E.R value. This is attributed to an overall reduction in flammable gas H_2 at ER 0.27 and an upsurge in concentrations of non-combustible gases like N_2 and CO_2. It has been noted that the lower heating value increases in line with an increase in the E.R. value. The LHV for the 0.15 E.R. is 4.764 MJ/Nm^3, while the greatest value for this study is 6.534 MJ/Nm^3 for the 0.22 E.R. Similar behavioural pattern was observed in the literature. [Upadhyay, D. 2018] The LHV value then drops once further for the E.R. 0.27, reaching 5.481 MJ/Nm^3. It results from a decrease in flammable gas H_2 at ER 0.27 and an increase in non-combustible gas concentrations such N_2 and CO_2. On the other hand, it was discovered that the patterns of CO and CH_4 concentrations were nearly consistent.

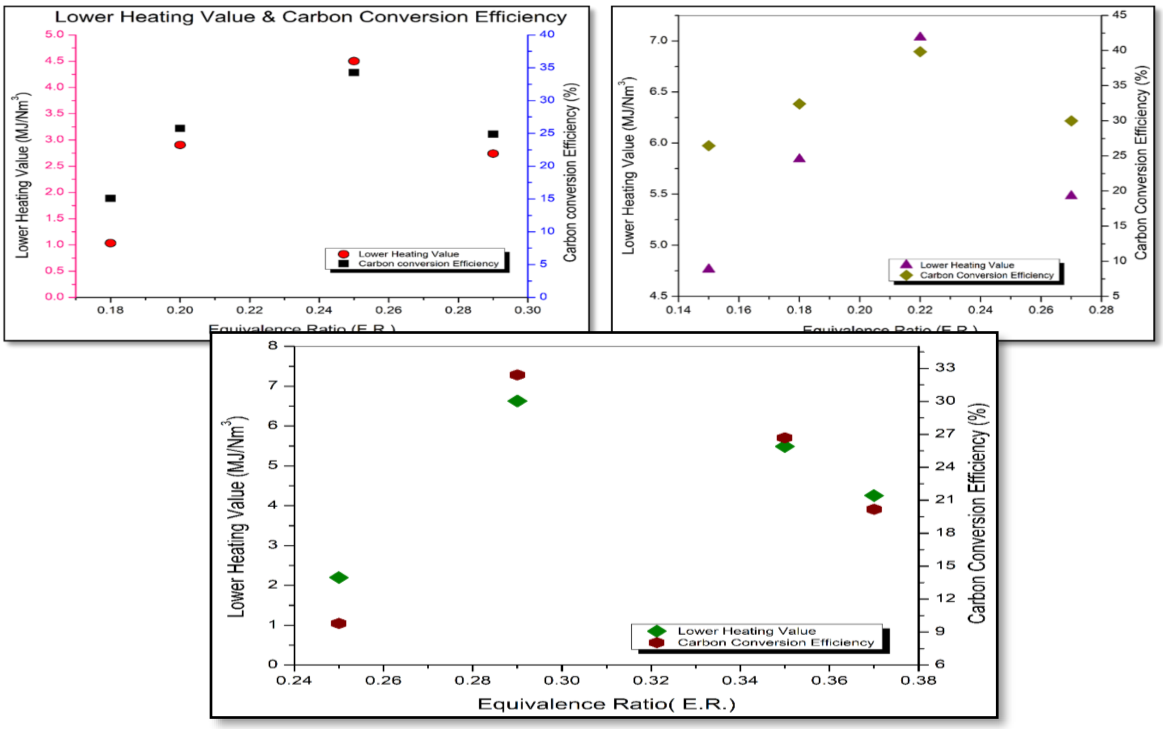

Figure 8: Lower Heating Value and Carbon Conversion Efficiency for Rice Husk, Sugarcane Bagasse and Pinewood samples.

6.5 Characterization of produced gasified char/ash:

6.5.1 Proximate Ultimate analysis of char/ash:

Samples Ultimate & Proximate Analysis													
Sr. No.	**Sample ID**	**LOD (%)**	**Ash (%)**	**Volatile Matter (%)**	**Fixed Carbon (%)**	**C (%)**	**H (%)**	**N (%)**	**S (%)**	**O(%)**	**HHV (MJ/kg)**	**O/C**	**H/C**
1	**Char/Ash Sugarcane Bagasse**	4.150	10.690	69.010	16.150	62.560	1.620	0.600	0.266	45.644	15.263	0.730	0.026
2	**Char/Ash Pinewood**	3.690	14.900	53.520	27.890	61.110	1.900	0.720	0.013	21.357	19.557	0.349	0.031
3	**Char/Ash Rice Husk**	2.400	77.020	15.520	5.060	8.190	3.080	0.320	0.029	11.361	5.165	1.387	0.376
4	**75 % R.H +25% O.W(A+) Char/ash**	0.36	65.96	4.42	29.26	38.8	0.239	6.08	0.187	54.695	3.603	1.410	0.006
5	**50% R.H + 50% O.W(B+) Char/ash**	0.650	63.920	5.600	29.830	54.400	0.289	6.947	0.505	37.859	11.987	0.696	0.005
6	**25% R.H + 75% O.W(C+) Char/ash**	0.640	60.830	6.430	32.100	67.600	0.394	6.470	0.607	24.929	18.935	0.369	0.006
7	**60% R.H + 40% O.W(D+) Char/ash**	0.670	61.110	5.810	32.410	52.800	0.283	6.901	0.507	39.509	11.140	0.748	0.005

Table 10: Proximate and Ultimate analysis of produced Char/Ash.

The proximate analysis of char/ash indicates that while Sugarcane Bagasse and Pinewood ash are not converted, Rice Husk ash is produced. This is because of limitations in the downdraft gasifier's equipment, such as incorrect air inlets and insufficient Gasification zones during the reaction. One disadvantage is the high degree of ash discovered in the proximate analysis of Sugarcane Bagasse char, Pinewood, and raw ricehusk. When using this by-product in heat-generating machinery, it is vital to take this condition into consideration. This high ash level causes a number of problems for the equipment, including as ash deposition, slagging and fouling, efficiency losses, and higher maintenance costs. [J.I. Arranz et al., 2021] It has been discovered that there is a significant decrease in the value of ash content when compared to the raw samples of the mixture of Rice Husk and organic waste, which clearly illustrates the successful occurrence of the Gasification reaction. Furthermore, it is reinforced by employing the char/ash production's HHV values. In this case, the ash content decreases from sample A+ to sample D+ as the concentration of organic waste increases, whereas the HHV values show the reverse pattern.

6.5.2 TGA analysis of char/ash

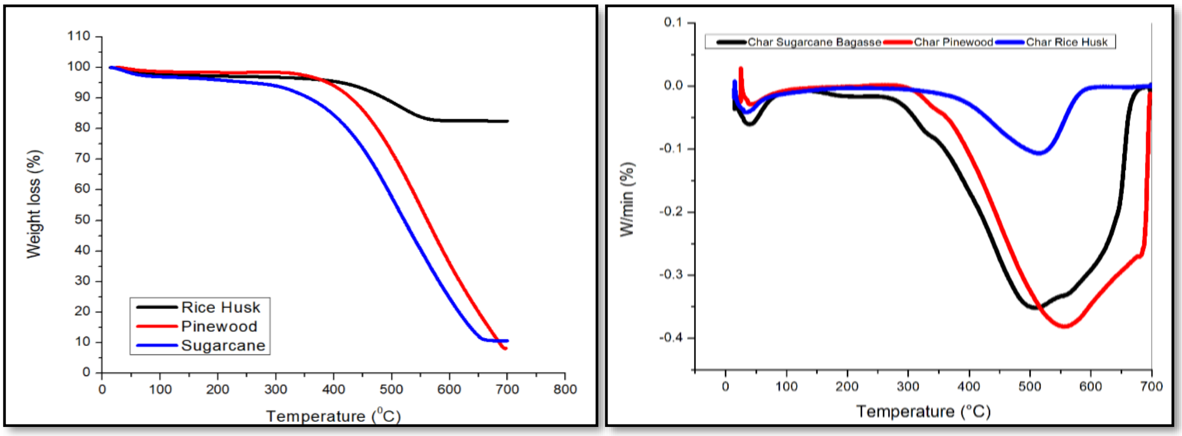

Figure 9: TGA and DTG graphs for the Char/ash produced from the Gasification of Rice Husk, Sugarcane Bagasse and Pinewood materials.

Furthermore, noted is the fact that, in both the proximate and ultimate analyses, only Rice Husk ash is formed, and while char is produced in both cases— or both Sugarcane Bagasse and Pinewood—a distinct pattern is also noted for Rice Husk. The mass loss for Rice Husk ranges from 100% to 82.9%, whereas the mass loss for sugarcane and Pinewood is documented as 100 to 10.66% and 100 to 8.16%, respectively. Additionally, it is seen that there is a substantial disparity in the loss of mass of the raw Rice Husk and Rice Husk ash. This is due to the fact that, following successful and sufficient Gasification, the only by-product that is created is ash, which has no weight loss and no burning potential. For the raw Rice Husk the mass loss reported from the 100% to 28%. On the other hand, the mass loss difference between raw Sugarcane Bagasse and Sugarcane Bagasse char is from 100% to 17% and from 100% to 10%, respectively, and between raw Pinewood and Pinewood char is from 100% to 12% and from 100% to 8.16%, respectively, because of insufficient air inlet and limitations of the downdraft gasifier. Figure displays the derivative thermogravimetry curves (DTG) for Rice Husk, Pinewood, and Sugarcane Bagasse. As can be observed, all of the samples' curves were similar, with a small peak in the beginning, a larger peak in the middle temperatures range, and a lengthy end peak that is almost 500 ^{0}C.

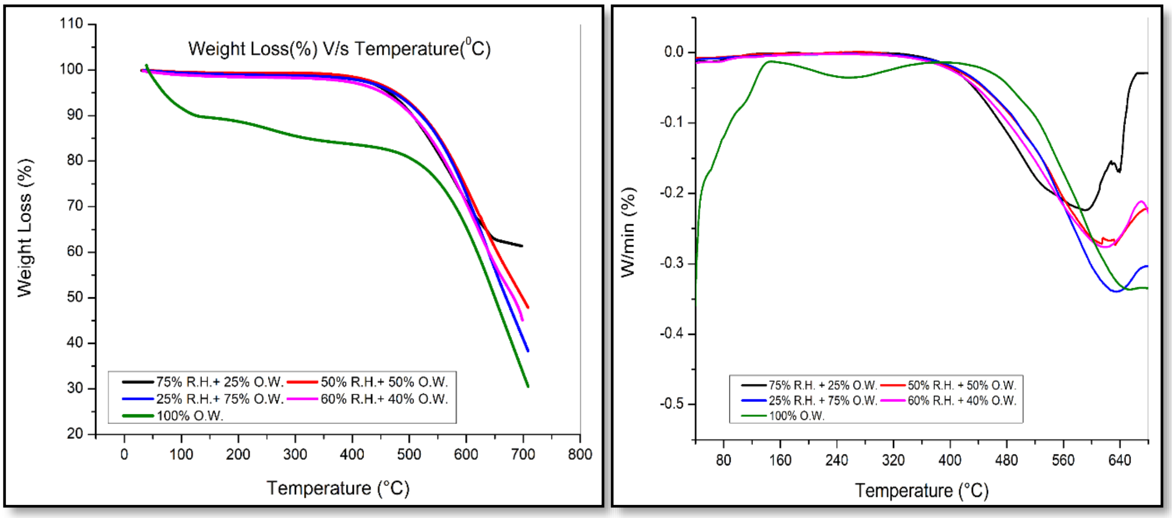

Figure 10: TGA and DTG graphs for the Char/ash produced from the Gasification of Rice Husk and organic waste and their different proportion samples.

6.5.3 Particle Size analysis of char/ash

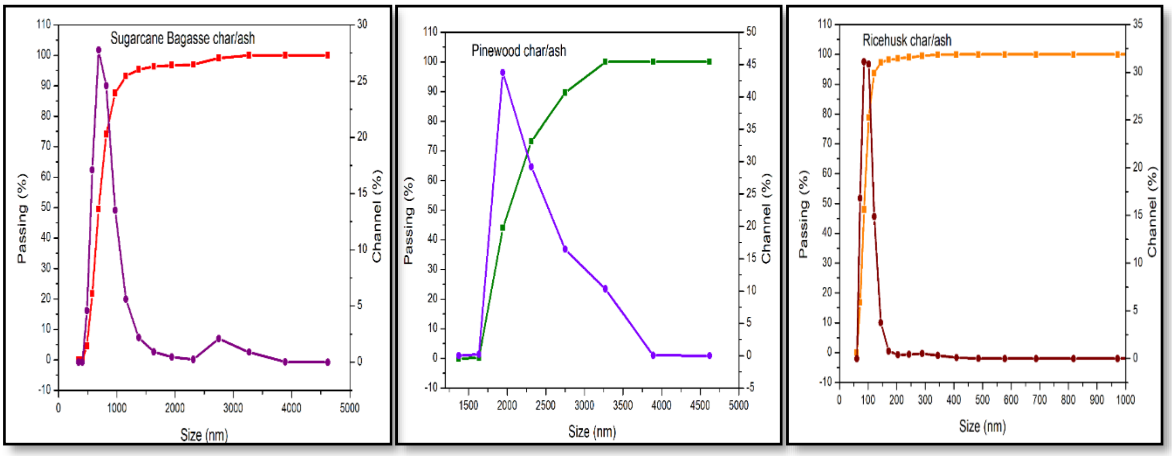

Figure 11: Particle Size analysis for the char/ash produced from the Gasification of the Sugarcane Bagasse, Pinewood and Rice Husk samples.

As seen in pictures, all three samples char/ash have been undergone for the particle size analysis.It has been observed that as Rice Husk ash is generated the material is passed from the 6540 nm to 72.30 nm and having the material passed from 100% to 16.79% and measured zeta potential for the Rice Husk is (-11.81mV). It has been observed that as Pinewood char is generated the material is passed from the 6540 nm to 1635 nm and having the material passed from 100% to 44 % and measured zeta potential for the Pinewood is (-5.88mV). It has been observed that as Sugarcane Bagasse char is generated the material is passed from the 6540 nm to 486 nm and having the material passed from 100% to 4.58 % and measured zeta potential for the Sugarcane Bagasse is (5.95mV).

6.5.4 Fourier transform infrared (FTIR) spectroscopy analysis:

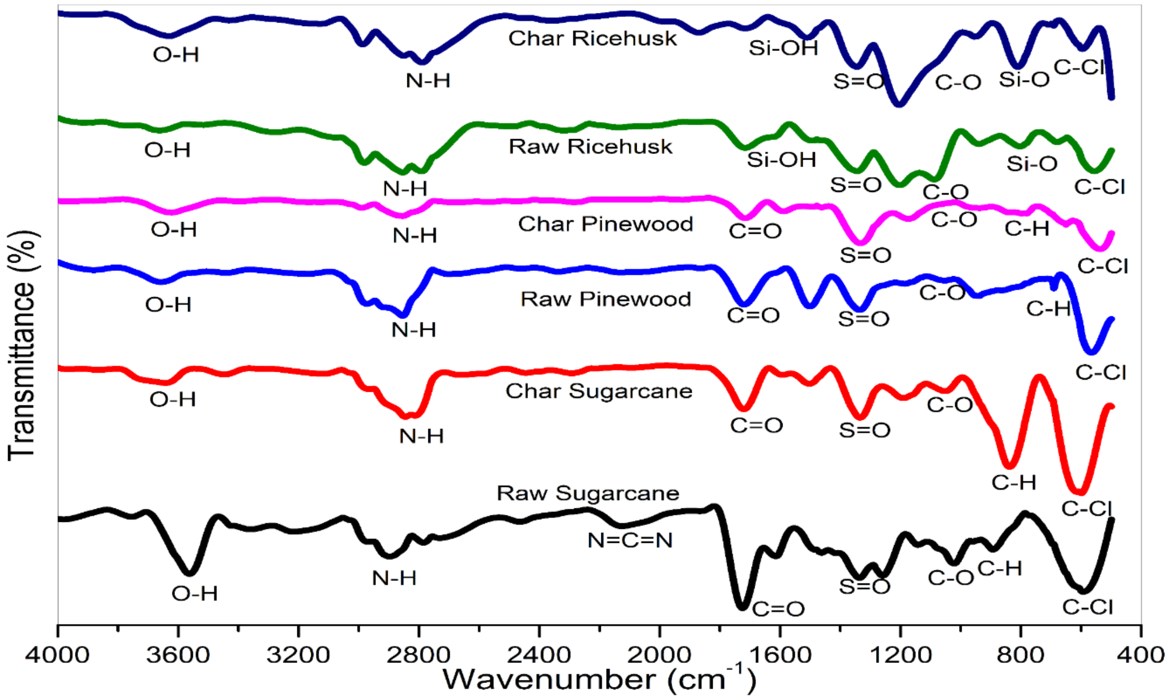

Figure 12: FTIR for all the raw and char/ash samples.

The peaks located between 3547 and 3624 cm^{-1} are indicative of free O–H stretching(alcohol) in the all of samples, which is linked to the breakdown of cellulose and hemicellulose which is in accordance with [Santos, V.C et al. 2022]. A similar pattern is also seen in [Darusman, D. et al. 2022] with regard to Pinewood material for both raw and char/ash Pinewood. For the Rice Husk samples, a comparable response was also observed with Pinewood and Sugarcane Bagasse. For every sample, the peaks ranging from 2783 to 2897 cm^{-1} indicate that N constrained N-H stretching (Primary amines (R-NH_2)). The peaks seen at 1710 - 1728 cm^{-1} can be ascribed to C = C and C = O, mainly to the aldehydes and ketones produced when all samples's cellulose and hemicellulose separate. The peaks of the Pinewood sample are 1629 and 1622 cm^{-1}, which corresponds with previous research [Darusman, D. et al. 2022]

Functional groups containing carboxylic acid (1600–1735 cm^{-1}), ketones, esters, and aldehydes. It's crucial to remember that natural biomass materials like Rice Husk, Pinewood, and Sugarcane Bagasse don't normally possess C-Cl and S=O bonds. It can be a sign of external pollution or chlorinated chemical treatment. Pesticides, preservatives, and other substances that could have come to contact with the biomass during cultivation, processing, or storage are potential sources of C-Cl and S=O bonds in the samples. The purpose of the Gasification process is to turn the residual carbon in the ash into CO_2 and remove materials from Rice Husks, such as cellulose, lignin, and hemicellulose.

It is anticipated than the ash will include SiO_2 because hydrogen gas turns into H_2O and silicon into SiO at high temperatures, while CO_2 and H_2O gasses evaporate. [Mujiyanti, D et al. 2021] It is evident that the peak at 3600 cm^{-1}, for both raw and ash Rice Husk, indicates the existence of free hydroxyl groups. Furthermore, the peaks at 1710 cm^{-1} for both samples demonstrated the C=O stretching, which is related to the aromatic groups in lignin and hemicelluloses. [Daffalla et al, 2010] peaks from 801 to 809 cm^{-1}, demonstrating the Si-O symmetric stretching vibration from Si-O-Si [D. Mujiyanti et al, 2021]

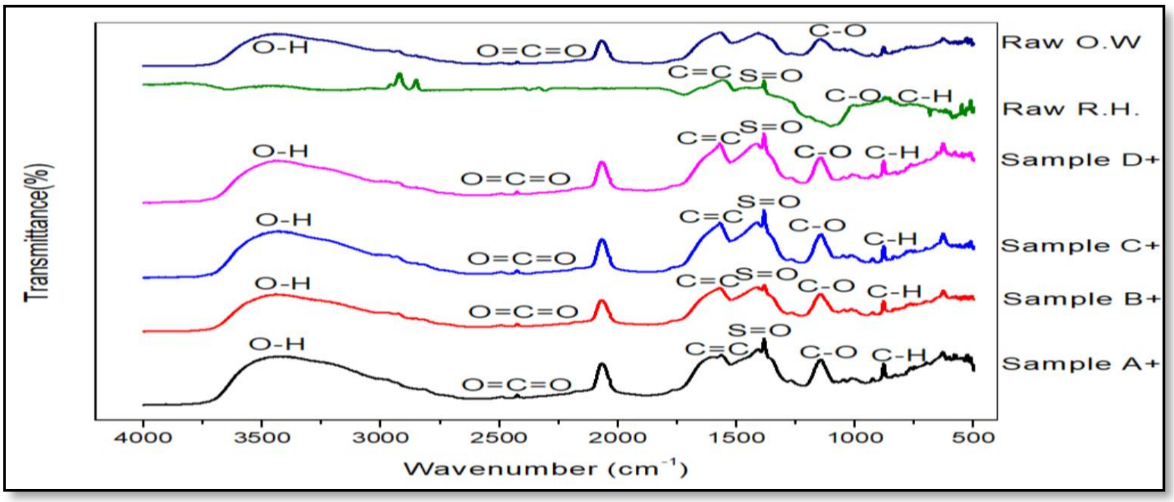

Figure 13: FTIR graphs of Rice Husk and organic waste and their different proportion samples

6.5.5 X-ray diffraction (XRD) analysis

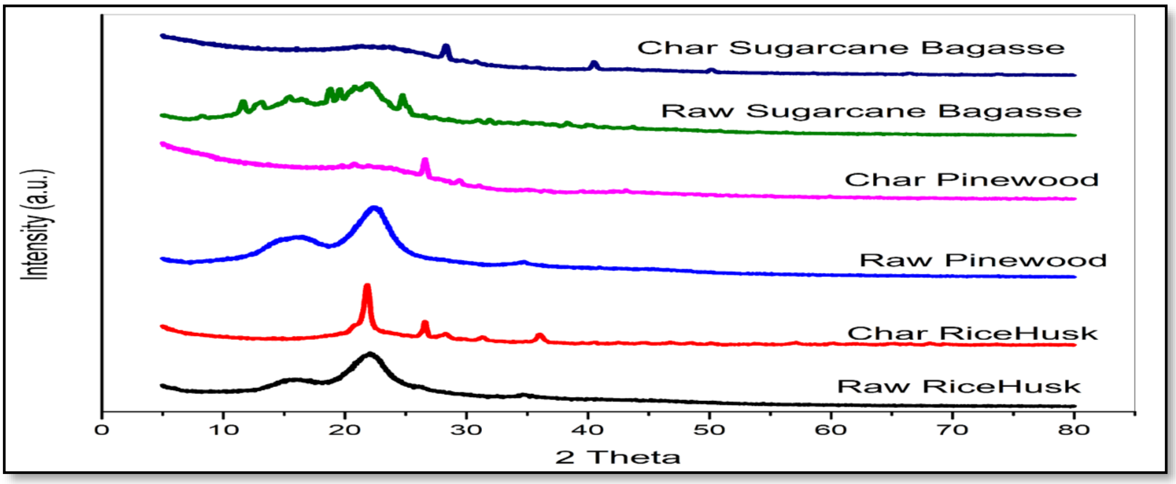

Figure 14: XRD for all the raw and char/ash samples.

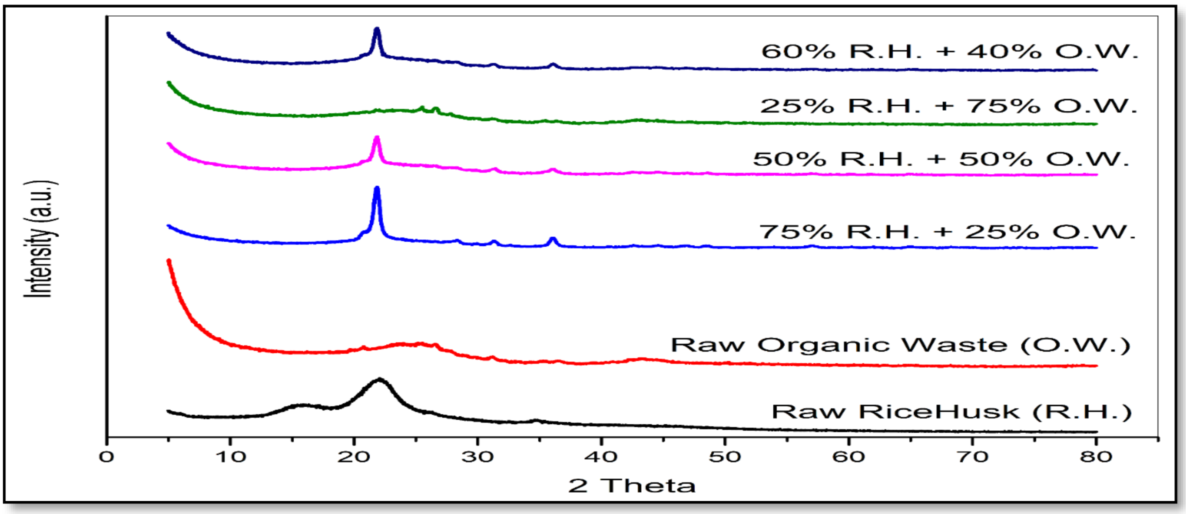

Figure 15: XRD graphs of Rice Husk and organic waste and their different proportion samples

6.5.6 X-ray Fluorescence (XRF) analysis

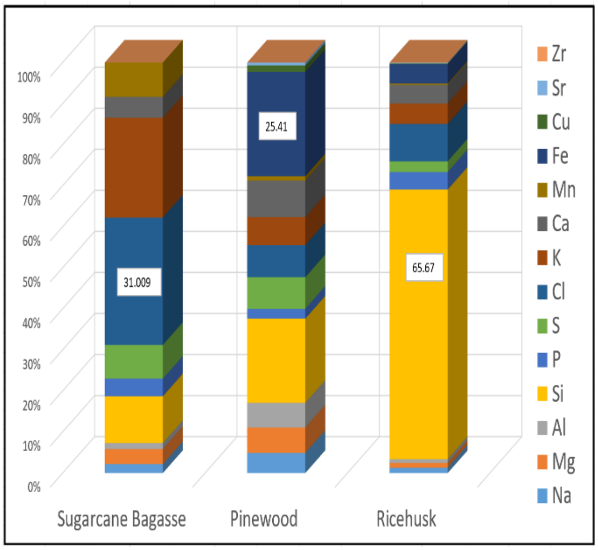

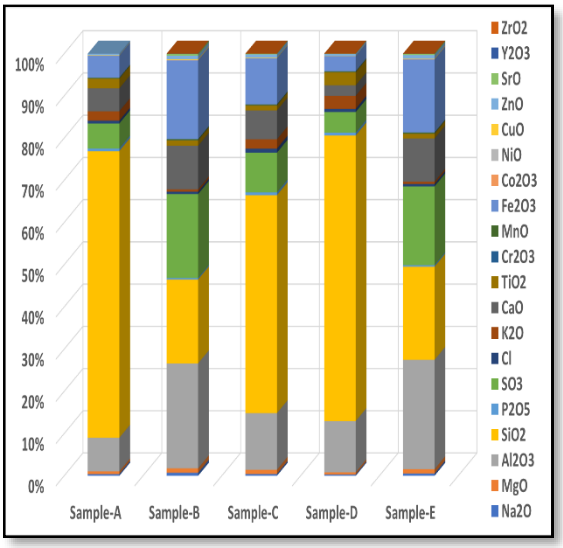

Figure 16: XRF analysis for the Sugarcane Bagasse, Pinewood and Rice Husk char/ash.
Figure 17: XRF analysis for the all five samples.

Analysis using X-ray fluorescence (XRF) was used to identify the main metals and other element concentrations. In theory, XRF is only sensitive and accurate when it comes to identifying relatively heavy metals in sufficiently high concentrations. The element contained in the char/ash samples of all three components is seen in the X-ray fluorescence analyses depicted in the figure. Using the XRF approach, thirteen elements were found like Na, Mg, Al, Si, P, S, Cl, K, Ca, Mn, Fe, Cu, Sr, Zr overall, albeit at slightly different amounts. Zr had the lowest concentration across all samples, with Cl being 31.009, Fe being 25.41, and Si being 65.67 in Sugarcane Bagasse, Pinewood, and ricehusk, respectively. The concentration of several components yielded results for Rice Husk consistent with this study [Khoo, Y. C. et al. 2013]. Si concentration is 65.67 whereas it is 63.766 in the paper; Al concentration is 0.899 when it is 0.73 in the article, and so on. Also from the analysis, it is observed that for the Sugarcane Bagasse char has the similar nature and concentration of the various component which has presented in the [Ullah, Z. 2020]. The presence of additional elements such as Fe, Sr, and Cu in Sugarcane Bagasse, Pinewood, and Rice Husk char/ash can be attributed to a variety of factors, including natural occurrences, contamination of the soil, soil chemistry, climatic circumstances, fertilizer type, processing, and handling. [G. D. Adamu et al., 2021] Cl > K > Si > Mn > S > Ca > P > Mg > Al > Na > Al; Fe > Si > Ca > Cl > S > K > Mg > Al > Na > P > Cu > Mn > Sr, and Si > Cl > K > Fe > Ca > P > S > Al > Na > Mg > Al > Mn > Cu > Zr are the concentrations of different components for Sugarcane Bagasse, Pinewood, and Rice Husk, respectively.

X-ray fluorescence (XRF) analysis was utilized to determine the amounts of additional elements and primary metals. Theoretically, only relatively high quantities of relatively heavy metals may be identified by XRF with appropriate sensitivity and accuracy. The X-ray fluorescence analyses shown in the picture show the element present in the char/ash samples of all five components. Because the Rice Husk sample also has the highest concentration of silica and its oxide, it was found that the presence of silica in its oxide form is highest in all five samples. In addition, it is observed that sample A, which has the largest percentage of Rice Husk (75%), also has the highest values of silica. Sample D, which has

60%, sample B, which has 50%, and sample C, which has 25%, all have silica values that have decreased to a substantial degree.

6.6 Waste Water analysis with basic parameters:

Sr. No.	Parameters	Unit	Ricehusk	Pinewood	Sugarcane Bagasse
1	pH	-	4.89	4.77	5.56
2	COD	mg/l	13583	12677	2587
3	Acidity	mg/l	1116	1442	233
4	Alkalinity	mg/l	BDL	BDL	BDL
5	Color	pt-co	2381	1738	2683
6	BOD	mg/l	6000	4560	2160

Table 11: Waste water analysis for the Rice Husk, Sugarcane Bagasse and Pinewood samples.

Sr. No.	Parameters	Unit	Sample A+	Sample B+	Sample C+	Sample D+
1	pH	-	4.37	4.06	4.07	6.04
2	TDS	mg/l	2437	2343	2372	1473
3	COD	mg/l	7750	8750	9500	3500
4	BOD	mg/l	3900	4650	5100	1900

Table 12: Waste water analysis for the Rice Husk, organic waste and their different proportion samples.

7. Achievements with respect to objectives

Sr. No	Objectives	Achievement
1	Initially, design, procure and install any one type of the gasifier along with the gas clarifying system.	**Designed and procured the downdraft gasifier having 10 kWe capacity. Also, installed the gas clarifying system with panel to measure the temperature.**
2	Optimize the numerous parameters like amount of air requirement for the Gasification, pressure and temperature of Gasification, method involved (fluidized bed, fixed bed and other gasifier) and composition of mixed solid waste (like Biomass, agriculture waste, industrial organic waste).	**First, method is chosen as downdraft gasifier. To optimize various parameters, three different biomass samples were taken and different equivalence ratios were selected and found the several parameters like air and fuel consumption rates, lower heating values, carbon conversion efficiency, energy content of producer gas and producer gas flow rate.**
3	Find out the best possible characteristics of Raw material like optimum composition of mixed waste, calorific value, bulk density and other basic details which can be derived from the proximate and ultimate analysis.	**Carried out the proximate and ultimate analysis of the all the raw samples and for the produced char/ash samples. Also, performed various analytical techniques like particle size analysis, TGA, FTIR, XRD and XRF.**
4	Ensure the best use of the raw material sources and Gasification technology that are available to you in order to produce the highest quality Synthesis gas (Syn Gas), which has higher concentrations of CO and H_2 in its gas composition and is meant to guide any potential reduction in emissions, including emissions of nitrogen, sulfur, and chlorine compounds.	**Experimented all four different samples like Rice Husk, Pinewood, Sugarcane Bagasse and industrial organic waste and all check the feasibility of the Rice Husk and organic waste mixture.** **Concluded that Rice Husk is the most optimized fuel which gives good values of LHV and when it mixed with industrial organic waste it generates greater value of LHV.**
5	Detail Kinetic study of Gasification process for the given solid waste through different methodologies like model free and model fit methods.	**First, detail study of the Thermogravimetric analysis of all samples have been done and plot and other information gathered. Afterwards, four different kinetic methods like model fitting and model free methods (direct Arrhenius method, Coats-Redfern method, Flynn-Wall-Ozawa (FWO) method and Kissinger-Akahira-Sunose (KAS) method) were adopted to calculate the various kinetic parameters like apparent activation energy, ln A and other.**

8. Conclusion:

In order to produce syngas, soild waste is gasified. This is a potential solution to various environmental problems, including air pollution, soil and water contamination, and the release of greenhouse gases. The goal of the project is to produce useful syngas from organic wastes in order to lower emissions of greenhouse gases and the usage of fossil fuels. Proximate and ultimate analysis, thermogravimetric analysis, particle size analysis, Fourier transform infrared spectroscopy, X-ray diffraction, X-ray fluorescence analysis, and waste water analysis are only a few of the analytical techniques used in this research. The equivalence ratio of the char/ash produced is a crucial parameter that affects the Gasification temperature, composition of the syngas, lower heating value, carbon conversion efficiency, and producer gas flow rate.

The study also looks at the ideal degradation model and kinetic parametric research employing procedures like Kissinger-Akahira-Sunose (KAS), Flynn-Wall-Ozawa (FWO), and Coats-Redfern. Using different ratios of Rice Husk to industrial organic waste, the study also investigates the Co-Gasification of agricultural waste and industrial organic waste. The same analytical techniques are applied to the produced char/ash. This research aims to construct a thermodynamic and kinetic model for future investigations and focuses on combining waste materials such as Rice Husk and industrial organic waste to produce Syngas. Among the goals are the design, procurement, and installation of gasifiers and gas clarifying systems, as well as the optimization of air needs, pressure, temperature, technique, and mixed solid waste composition.

The study also seeks to identify the ideal raw material properties and Gasification technique for producing syngas with increased CO and H_2 concentrations and possible emission reduction. Using model-free and model-fit techniques, the study also looks at the kinetic analysis of the Gasification process for solid waste.

9.List of all publications arising from the thesis:

9.1 Journal Publication

Endrick D. Contractor, Kushal P. Mehta, Aditi Thattil, Alok Gautam, Shina Gautam (2024), "Detailed Analysis of Downdraft Gasifier Using Different Parameters For Biomass Gasification: A Review", Energy. Environment. Efficiency. Resources. Globalization (EMERG), Volume X, Issue 1/2024, ISSN 2668-7003, ISSN-L 2457-5011, pp 94 – 117, DOI: 10.37410//EMERG.2024.1.07

9.2 Conference proceeding

Endrick Contractor, Harsh Patel, Alok Gautam, Shina Gautam, "Gasification of High Calorific Content in MSW", Green Technologies for Sustainable Development 2021, 1st Edition, ISBN: 978-93-5457-142-8, 384-394, DHARMSINH DESAI UNIVERSITY(DDU), Nadiad, March 2021.

10. Reference:

A.A. P. Susastriawan, Harwin Saptoadi & Purnomo (2019): Utilization of Rice Husk–sawdust as blending feedstock of small-scale downdraft gasifier, Energy Sources, Part A: Recovery, Utilization, and Environmental Effects, DOI: 10.1080/15567036.2019.1600620

Adamu G. D. et al, (2021), "Elemental Analysis of Rice Husk Using X-Ray Fluorescence Techniques – A Case Study of Jigawa State, Nigeria", Dutse Journal of Pure and Applied Sciences (DUJOPAS), Vol. 7 No. 4b December 2021, https://dx.doi.org/10.4314/dujopas.v7i4b.17

Awais, M., Li, W., Munir, A., Omar, M. M., & Ajmal, M. (2020). Experimental investigation of downdraft biomass gasifier fed by Sugarcane Bagasse and coconut shells. Biomass Conversion and Biorefinery. doi:10.1007/s13399-020-00690-5

Daffalla, Samah & Mukhtar, Hilmi & Shaharun, Maizatul. (2010). Characterization of Adsorbent Developed from Rice Husk: Effect of Surface Functional Group on Phenol Adsorption. Journal of Applied Sciences. 10.3923/jas.2010.1060.1067.

Darusman, D., Syakur, S., Kurniasih, E.M., Puspita, V., & Zaitun, Z. (2022). Functional Group Structure of Bamboo and Pine Wood Biochar Due to Differences in Pyrolysis Temperature. Aceh International Journal of Science and Technology.

Havilah, P.R.; Sharma, A.K.; Govindasamy, G.; Matsakas, L.; Patel, A. (2022) Biomass Gasification in Downdraft Gasifiers: A Technical Review on Production, Up-Gradation and Application of Synthesis Gas. Energies 2022, 15, 3938. https://doi.org/10.3390/en15113938

J. Bonilla et al.(2019) "Kinetic triplet of Colombian sawmill wastes using thermogravimetric analysis", Heliyon 5 (2019) e02723https://doi.org/10.1016/j.heliyon.2019.e02723

J.M. Criado, J. Morales (1977), Thermal decomposition reactions of solids controlled by diffusion and phase-boundary processes: possible misinterpretation of the mechanism from thermogravimetric data, Thermochim. Acta. 19 305–317. https://doi.org/10.1016/0040-6031(77)80006-3.

Jahromi R, Rezaei M, Samadi SH. (2020) Sugarcane Bagasse Gasification in a Downdraft Fixed-Bed Gasifier: Optimization of Operation Conditions. ChemRxiv. 2020; doi:10.26434/chemrxiv.12361031.

Khoo, Y. C., Johari, I., & Ahmad, Z. A. (2013). Influence of Rice Husk Ash on the Engineering Properties of Fired-Clay Brick. Advanced Materials Research, 795, 14–18. doi:10.4028/www.scientific.net/amr.795.14

Kyriaki, Trouli., S.N., Dokianakis., E., Vasilaki., N., Katsarakis. (2023). Treatment of Agricultural Waste Using a Combination of Anaerobic, Aerobic, and Adsorption Processes. Sustainability, doi: 10.3390/su15031892.

Moretti, M.M.de S., et al. (2016) Effect of pretreatment and enzymatic hydrolysis on the physical-chemical composition and morphologic structure of Sugarcane Bagasse and sugarcane straw. Bioresour. Technol. (2016)http://dx.doi.org/10.1016/j.biortech.2016.08.075

Motta, I. L., Miranda, N. T., Maciel Filho, R., & Wolf Maciel, M. R. (2019). Sugarcane Bagasse Gasification: Simulation and analysis of different operating parameters, fluidizing media, and gasifier types. Biomass and Bioenergy, 122, 433–445. doi:10.1016/j.biombioe.2019.01.051

Mujiyanti, D.; Ariyani, D.; Lisa, M. Silica Content Analysis of Rice Husks Siam Unus from South Kalimantan. Indo. J. Chem. Res. 2021, 9, 81-87. DOI: https://doi.org/10.30598//ijcr.2020.9-muj

Santos, V.C., Lima, Á.S., Soares, C.M., & Souza, R.L. (2022). FTIR And TGA/DTG Characterization Of Sugarcane Waste. Blucher Engineering Proceedings.

Svishchev, D. (2022). Experimental Study to Replicate Wood Fuel Conversion in a Downdraft Gasifier: Features and Mechanism of Single Particle Combustion in an Inert Channel. *Applied Sciences*, *12*(3), 1179. https://www.mdpi.com/2076-3417/12/3/1179

Tolu Emiola-Sadiq, Lifeng Zhang, and Ajay K. Dalai (2021), “Thermal and Kinetic Studies on Biomass Degradation via Thermogravimetric Analysis: A Combination of Model-Fitting and Model-Free Approach”, https://doi.org/10.1021/acsomega.1c02937 ACS Omega 2021, 6, 22233−22247.

Ullah, Z. (2020). Synergistic effect of Sugarcane Bagasse ash and marble sludge powder as a partial replacement of cement in concrete. Journal of mechanics of continua and mathematical sciences.15. 12-26

Upadhyay, D. S., Sakhiya, A. K., Panchal, K., Patel, A. H., & Patel, R. N. (2018). Effect of Equivalence Ratio on the Performance of the Downdraft Gasifier – An Experimental and Modelling Approach. Energy. doi:10.1016/j.energy.2018.11.133

Yan Cao*, Yu Bai, Jiang Du(2021), Air-Gasification of pine sawdust using dolomite as in-bed material: Effects of Gasification conditions on product characteristics, Journal of the Energy Institute, Volume 95, 2021, Pages 187-192, ISSN 1743-9671, https://doi.org/10.1016/j.joei.2021.01.010.

Zhao, S., Bi, X., Pan, X., Su, Y., & Wu, W. (2019). The optimization of in-situ tar reduction and syngas production on a 60-kW three-staged Biomass Gasification system: a theoretical and practical approach. Biomass Conversion and Biorefinery. doi:10.1007/s13399-019-00536-9